Controlling intermolecular spin interactions of La@C_{82} in empty fullerene matrices†

Yasuhiro Ito,*[a] Jamie H. Warner,[a] Richard Brown,[a] Mujtaba Zaka,[a] Rudolf Pfeiffer,[b] Takayuki Aono,[c] Noriko Izumi,[c] Haruya Okimoto,[c] John J. L. Morton,[ad] Arzhang Ardavan,[d] Hisanori Shinohara,[c] Hans Kuzmany,[b] Herwig Peterlik[b] and G. Andrew D. Briggs[a]

Received 8th July 2009, Accepted 3rd December 2009
First published as an Advance Article on the web 8th January 2010
DOI: 10.1039/b913593f

The ESR properties and crystal structures of solid-state La@C_{82} in empty fullerene matrices were investigated by changing the concentration of La@C_{82} and the species of an empty fullerene matrix: C_{60}, C_{70}, $C_{78}(C_{2v}(3))$, $C_{82}(C_2)$ and $C_{84}(D_{2d}(4))$. The rotational correlation time of La@C_{82} molecules tended to be shorter when La@C_{82} is dispersed in larger fullerene matrices because large C_{2n} molecules provide more space for La@C_{82} molecules for rotating. La@C_{82} dispersed in a hcp-C_{82} matrix showed the narrowest hyperfine structure (hfs) due to the ordered nature of La@C_{82} molecules in the C_{82} crystal. On the other hand, in a C_{60} matrix, La@C_{82} molecules formed clusters because of the large different solubility, which leads to the ESR spectra being broad sloping features due to strong dipole–dipole and exchange interactions.

1. Introduction

Mono-metallofullerenes (MFs) M@C_{82} (M = Sc, Y and La) and endohedral nitrogen fullerene N@C_{60} have appealing electron spin states and magnetic properties which have a potential for solid-state quantum information processing (QIP) and spintronics.[1–3] The associated radical electron spins on the C_{82} cage or nitrogen atom in C_{60} cage have been shown to possess long T_1 and T_2 times.[3–9] Fullerenes are almost spherical molecular structures and can be arranged in one-, two- or three-dimensional arrays[1,10–12] which are very promising as building blocks for compact solid-state carbon-based architectures.

Since their discovery in 1991, the magnetic properties of solution and solid state mono-MFs have been the subject of much investigation. The electron spin resonance (ESR) spectra of M@C_{82} in solution can be identified by its hyperfine interaction with I = 7/2 of ^{45}Sc,[4,13–16] 1/2 of ^{89}Y[17,18] and 7/2 of ^{141}La.[4,15,19–22] The magnetic properties of pure solid-state Sc@C_{82} and La@C_{82} powders have been studied using ESR and superconducting quantum interference device (SQUID) magnetic measurements.[23,24] The temperature dependent ESR and magnetic susceptibilities of Sc@C_{82} and La@C_{82} powder samples exhibit changes in the magnetic behaviour between 100 and 200 K due to a structural phase transition related to uniaxial molecular rotation.[24,25] However, hfs has not been reported in pure crystal powders due to the presence of the exchange and dipole–dipole interaction between M@C_{82} molecules. A key step in utilizing spin-active endohedral fullerenes in solid-state architectures is the understanding of the behaviour of isolated spins in the solid state, and the ability to control spin–spin interactions.

Recently, Jakes *et al.* reported that the hfs of La@C_{82} dispersed in a solid C_{60} matrix can be measured.[26] However, the hfs in this case was not as well resolved as one might expect from well-isolated spins, presumably due to a combination of residual exchange and dipole–dipole interactions. This indicates that La@C_{82} molecules formed cluster-like structures and were not well isolated. C_{60} may not be the ideal matrix to disperse mono-MF due to the mismatch in cage sizes and shapes. Larger cage structures such as C_{78}, C_{80}, C_{82} and C_{84} may provide better dispersion of the mono-MFs and enable the solid-state electron spin properties of well-dispersed mono-MFs to be revealed.

Here, we report the concentration dependent ESR properties and hfs of La@C_{82} diluted in a variety of empty fullerene (C_{2n}) matrices: $C_{60}(I_h)$, $C_{70}(D_{5h})$, $C_{78}(C_{2v}(3))$, $C_{82}(C_2)$[27] and $C_{84}(D_{2d}(4))$.[28] We examine concentrations in the range of 0.1–1 mol% in order to explore the highly diluted regime necessary to obtain isolated spins. We find that the intermolecular dipole–dipole interaction between La@C_{82} molecules can be controlled by changing the concentration of La@C_{82} and the cage size of the empty fullerene matrix. For cage sizes larger than C_{60}, we find no evidence for cluster formation at 0.1 mol% La@C_{82} concentration. We correlate our ESR studies with structural analysis using X-ray diffraction (XRD)

[a] *Department of Materials, Quantum Information Processing Interdisciplinary Research Collaboration (QIP IRC), University of Oxford, Parks Rd, Oxford, UK OX1 3PH. E-mail: yasuhiro.ito@materials.ox.ac.uk*
[b] *University of Vienna, Faculty of Physics, Strudlhofgasse 4, A-1090, Vienna, Austria*
[c] *Department of Chemistry and Institute for Advanced Research, Nagoya University, Furo-Cho, Chikusa-ku, 464-8602, Nagoya, Japan*
[d] *Centre for Advanced Electron Spin Resonance (CAESR), Clarendon Laboratory, Department of Physics, University of Oxford, Parks Rd, Oxford, UK OX1 3PU*

† Electronic supplementary information (ESI) available: Numerical data of ESR simulation and crystal structures for C_{2n} powder with La@C_{82}, schematic models of La@C_{82} in C_{2n} fcc-crystals, ESR simulation and results. See DOI: 10.1039/b913593f

and show that the crystal phase of the fullerene matrix plays an important role in the spin properties, such as spin relaxation.

2. Experimental

Empty fullerenes and La@C_{82} were produced by direct-current arc discharge of La_2O_3/graphite composite rods (Toyo Tanso Co., Ltd.) under helium flow at 80 Torr.[18] Fullerenes were extracted from the carbon soot by carbon disulfide and dimethylformamide. Pure empty fullerenes and La@C_{82} were isolated by high performance liquid chromatography (HPLC, LC-9103, Japan Analytical Industry Co., Ltd.) with three complementary 5PYE, Buckyprep and Buchyprep-M (Nacalai Tesque Co., Ltd.) columns. The purities of these fullerenes were confirmed by laser-desorption time of flight (LD-TOF) mass spectroscopy.

Three kinds of concentration (0.1, 0.5 and 1 mol%) La@C_{82} samples in empty fullerene matrices in quartz tubes (3 mm inside diameter) were prepared by evaporating fullerene solutions in carbon disulfide after ten times of freeze-pump-thaw cycles and sealing under vacuum. ESR measurements were performed on an EMX X-band CW EPR spectrometer (Bruker Co., Ltd.) at room temperature. ESR spectra were simulated by the EasySpin software package.[30]

Pulsed ESR experiments were performed using an X-band (9–10 GHz) Bruker EPR spectrometer (Elexsys 580) with T_2 measured by a standard Hahn echo technique ($\pi/2$-τ-π-τ-echo, where τ is incremented) and T_1 by an inversion recovery experiment (π-τ-$\pi/2$-T-π-T-echo, where τ is incremented and T is short and fixed). The pulse lengths of $\pi/2$ and π were 80 and 160 ns for the 1 mol% samples, and 16 and 32 ns for the 0.1 mol% samples, respectively.

Characterization with X-rays was performed using a rotating anode generator (Cu Kα radiation collimated and monochromated from crossed Göbel mirrors, Nanostar, Bruker AXS, Karlsruhe), equipped with a pinhole camera and a 2D position sensitive detector (VANTEC2000, gas detector with microgap technology). All X-ray patterns were radially averaged and corrected for background scattering to obtain the scattering intensity in dependence on the scattering vector q, where $q = 4\pi\sin\theta/\lambda$ with 2θ being the scattering angle and $\lambda = 0.1542$ nm the X-ray wavelength. The specimens were measured in transmission at a sample to detector distance of 13 cm and a measuring time of either 2 or 6 h. Measurements were performed at least at two different positions of the crystal powder.

3. Results and discussion

3.1 ESR spectra measurements of La@C_{82} in C_{2n} matrices

If it is assumed that La@C_{82} molecules are uniformly dispersed in C_{2n} matrices (*i.e.* La@C_{82} molecules are located at the centre of C_{2n} fcc-crystals) then the average distance between La@C_{82} molecules can be varied between 4 to 9.5 nm as the concentration is varied from 1 to 0.1 mol% (Fig. S1, ESI†)[29] with a resulting influence on the magnetic interactions between La@C_{82} molecules. Fig. 1 shows the ESR spectra of La@C_{82} in 0.1, 0.5 and 1 mol% concentration in C_{2n} matrices (C_{60}, C_{70}, C_{78}, C_{82} and C_{84}) at room temperature accompanied by simulated spectra. The ESR spectra were simulated by taking into account the constant anisotropic g tensor (2.0021 2.0013 2.0010), a tensor (2.15 2.25 4.85), the rotational correlation time (4 ns), and different linewidth and exchange frequency (0.050 $\sim$ 0.102) (see Table S1, ESI).† The hfs of a radical electron on the C_{82} cage of La@C_{82} shows eight lines due to the hyperfine interaction with $I = 7/2$ of ^{141}La. Dipole–dipole interactions between La@C_{82} molecules will broaden the full width at half maximum (FWHM) of the hfs (Fig. 1 and S2b, ESI†).[30] In all cases, broader linewidths are observed at 0.5 and 1 mol% concentrations than that for 0.1 mol% concentration. This broadening stems from increasing dipole–dipole interactions between La@C_{82} molecules, due to the average distances between La@C_{82} molecules in 0.5 and 1 mol% concentrations being about 4.1 and 5.3 nm less than that in 0.1 mol% concentration, respectively (Fig. S1).† The sample of 0.1 mol% La@C_{82} in C_{82} matrix gives the narrowest linewidth, indicating that La@C_{82} molecules are well dispersed in the C_{82} matrix. Furthermore, the ESR spectra of La@C_{82} in 0.5 and 1 mol% concentrations in a C_{60} matrix show a sloping background across the hfs. The broad sloping features can be simulated by using a combination of strong exchange interactions and broad FWHM linewidth, indicating that La@C_{82} molecules form cluster-like structures in C_{60} matrix (see Fig. S2, ESI).†

3.2 Rotational correlation time analysis by Kivelson's equation

In order to obtain further information such as rotational properties of the electron spin behaviour of La@C_{82} molecules in C_{2n} matrices, we investigated the individual linewidths of the eight hyperfine peaks by fitting the integrated ESR spectra with Lorentzian curves. The linewidth $\Delta H_{1/2,\mathrm{I}}$ of the eight lines in the hfs can be fitted to Kivelson's equation:[31]

$$\Delta H_{1/2,\mathrm{I}} = k_0 + k_1 m_\mathrm{I} + k_2 m^2 + k_4 m_\mathrm{I}^4 \qquad (1)$$

where m_I is the nuclear spin quantum number. The concentration and matrix dependences of k_i against the molecular diameter of C_{2n} molecules are shown in Fig. 2. According to previous studies,[15] k_0 is related not only to the rotational correlation time but also to exchange and dipole–dipole interactions. k_0 in C_{70}, C_{78}, C_{82} (0.5 and 1 mol%) and C_{84} matrices depend on the concentration, suggesting that the dipole–dipole interactions between La@C_{82} molecules in these matrices can be controlled. However, k_0 in 0.1 mol% concentration in C_{82} matrix was lower than those in other fullerene matrices, which suggests that La@C_{82} molecules have weaker dipole–dipole interactions with other La@C_{82} molecules, or possibly a shorter rotational correlation time, (*i.e.* La@C_{82} molecules rotate faster than in other concentrations or matrices). k_0 in C_{60} matrix is the largest in all matrices, consistent with poor dispersion of La@C_{82} molecules in the C_{60} matrix and the resulting strong exchange and dipole–dipole interactions.

Information about the rotational behaviour of La@C_{82} molecules in C_{2n} matrices can be extracted from k_1,[15] as k_1 is independent of exchange and dipole–dipole interactions. Fig. 2b shows that the rotational correlation time tends to be shorter when La@C_{82} is dispersed in larger fullerene

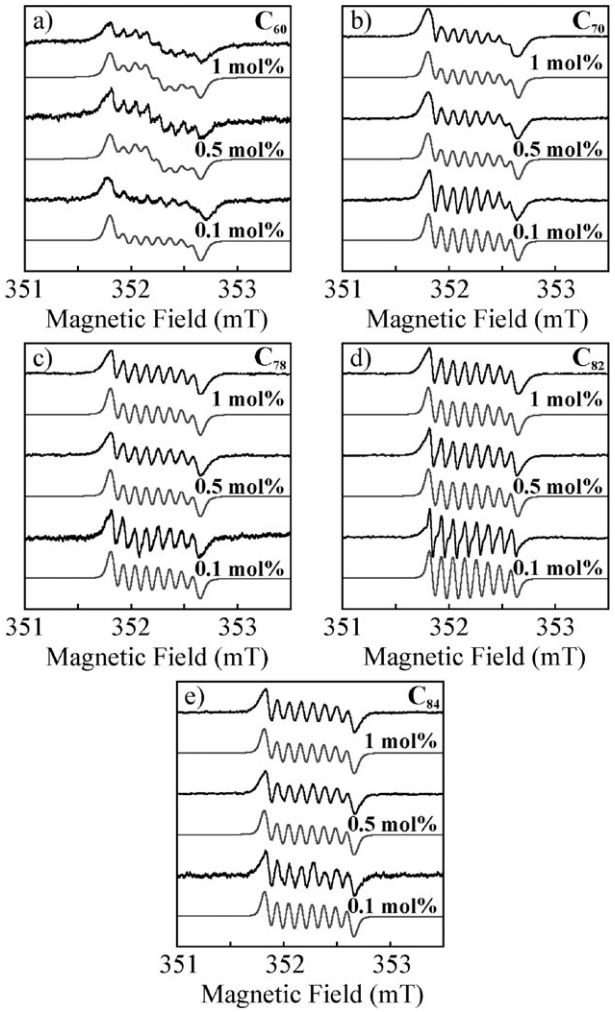

Fig. 1 ESR (black) and simulated ESR (gray) spectra of La@C_{82} in 0.1, 0.5 and 1 mol% in (a) C_{60}; (b) C_{70}; (c) C_{78}; (d) C_{82}; and (e) C_{84} matrices at room temperature. Microwave frequency, power and modulation amplitude are 9.867 GHz, 0.2 mW and 0.025 mT, respectively.

matrices, indicating that large C_{2n} molecules provide more space for La@C_{82} molecules to rotate. In the C_{60} matrix, La@C_{82} molecules rotate slowly because of the significant difference in cage size. The rotational correlation time τ_r can be calculated by follows:[26]

$$k_1 = \frac{1}{15}\frac{2}{3}\Delta g\frac{\mu_B B_0}{\hbar}\ \frac{2}{3}\Delta a\ \left[4\tau_r + \frac{3\tau_r}{1+(\omega\tau_r)^2}\right] \qquad (2)$$

where μ_B, B_0, $\hbar$, ω are Bohr magneton, the magnetic field, Planck's constant and the microwave frequency of measurements, respectively. Differences of principle values of the g matrix and the hfi tensor have been determined previously as $\Delta g = g_{\parallel} - g_{\perp} = 0.007$ and $\Delta a = a_{\parallel} - a_{\perp} = 5$ MHz.[15] The numerical data of the rotational correlation time is shown in Table S2 (ESI).† These values were 0.14 $\sim$ 0.52 ns which are close to the rotational correlation time by the spectral simulation (4 ns) and in agreement with the previous report (1.1 ns).[26] The slight difference may be due to some unspecified interactions such as π-orbital hybridization between La@C_{82} and C_{2n} molecules in the solid-state. We have to consider that k_4 in 0.5 and 1 mol% concentration in C_{60} matrix were positive, which are unphysical values. ESR spectra for 0.5 and 1 mol% concentration in C_{60} matrix are very difficult to analyze because of a sloping background structure which stems from strong exchange interaction and very broad hfs due to a strong dipole–dipole interaction. We examine the qualitative change in k_4, but do not extract any quantitative information due to the unphysical negative values.

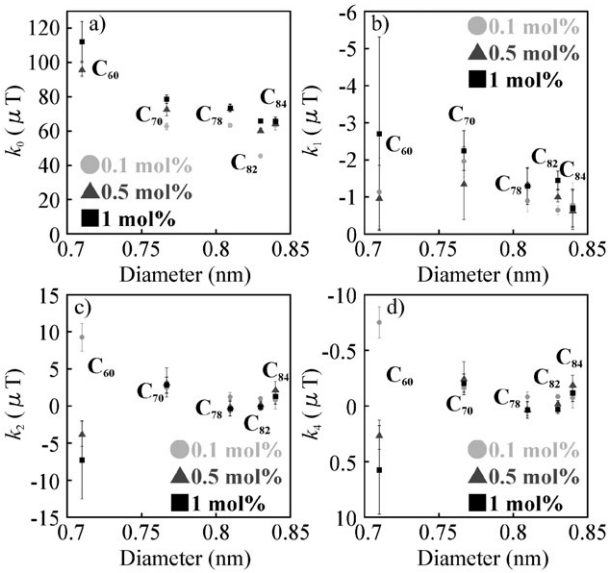

Fig. 2 Matrix dependence of the k_i values: (a) k_0; (b) k_1; (c) k_2; and (d) k_4. The horizontal axis is the diameter of empty fullerene molecules which is calculated by equation S4.

3.3 Spin relaxation time analysis of La@C_{82} in C_{2n} matrices

In order to confirm the existence of a cluster-like structure of La@C_{82} molecules in C_{60} matrix, we investigated the spin-lattice (T_1) relaxation time. Information regarding the spin relaxation properties can be obtained by power dependent saturation measurements of the ESR spectra which are obtained by recording the total integrated area at the microwave absorption from the ESR spectra as a function of the microwave power; we studied powers from 0.02 to 63.25 mW (0.14 to 7.95 $(mW)^{1/2}$). Fig. 3 shows the saturation curves of La@C_{82} in C_{60} and C_{82} matrices (Fig. S3 shows for C_{70}, C_{78} and C_{84}, ESI).† The saturation curves for the C_{70}, C_{78}, C_{82} and C_{84} matrices did not depend on the concentration and all showed saturation between 2–4 $(mW)^{1/2}$. This indicates that the time T_1 is similar for each concentration. T_1 and T_2 times can also be investigated by pulsed ESR measurements. We measured T_1 and T_2 times of 0.1 and 1 mol% in C_{82} matrix. T_1 time of 0.1 and 1 mol% were 876 and 751 ns and T_2 time were 674 and 385 ns, respectively. The relaxation time of 0.1 mol% sample was longer than 1 mol% sample. The longer spin relaxation time of La@C_{82} in 0.1 mol% in C_{82} matrix causes narrower hfi lines of CW ESR.

In the case of the C_{60} matrix, the curves for 0.5 and 1 mol% concentration were noticeably non-saturated, which indicates that the T_1 time of La@C_{82} in the C_{60} matrix is shorter than

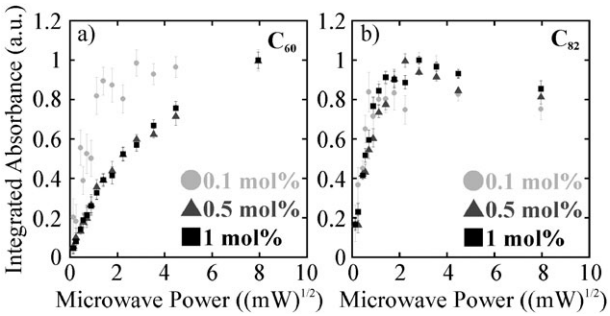

Fig. 3 Saturation curves of La@C_{82} in 0.1, 0.5 and 1 mol% in (a) C_{60}; and (b) C_{82} matrices at room temperature. The microwave frequency and modulation amplitude are 9.867 GHz and 0.025 mT, respectively.

those in other matrices. The curves for 0.5 and 1% concentrations were very different from those in other matrices. The difference in saturation curves stems not only from stronger dipole–dipole interactions but also from exchange interactions between La@C_{82} molecules in the cluster. This is confirmed by the microwave power dependent ESR spectra of La@C_{82} in C_{60}, shown in Fig. 4 (Fig. S4 shows for C_{70}, C_{78} and C_{84}, ESI).† The ESR spectra in 0.5 and 1 mol% in C_{60} matrix with 20 mW microwave power were different from those in other fullerene matrices. These spectra show the emergence of a peak in the central region associated with exchange narrowing in La@C_{82} cluster, that is, the spins with short T_1 in La@C_{82} cluster are picked at higher microwave power (Fig. S2).† Understanding the local physical environment surrounding the spin-active disordered La@C_{82} molecules in the solid-state crystals is important for correlating ESR with structure.

We measured the CW ESR spectra of La@C_{82} in C_{60} at concentrations from 1 to 60 mol%. At 60 mol% concentration, this ESR spectrum showed only one narrow peak due to strong exchange interactions occurring in the clusters. We were not able to get a Hahn echo signal from this sample. The presence of strong exchange interactions leads to the electrons being delocalized and consequently experiencing different local magnetic fields. Thus it is difficult to refocus delocalized electrons to obtain the Hahn echo signal. This makes it difficult to compare quantitatively T_1 and T_2 times of La@C_{82} in C_{60} and C_{82} matrices due to different degrees at clustering. Although we were able to get T_1 and T_2 times at low concentrations from 0.1 to 1 mol%, these values may not be representative of the ensemble and instead we believe power dependent saturation curve measurements are adequate to compare the changes of the T_1 and T_2 times for La@C_{82} in different matrices.

3.4 Crystal structure analysis of C_{2n} solid with La@C_{82} molecules

The crystal structure of the fullerene solids was examined using XRD. Fig. 5 shows the X-ray diffraction patterns of the solid powder of C_{2n} molecules with La@C_{82}. The numerical data of the crystal structure are shown in Table S2 (ESI).† The diffraction patterns of C_{78} and C_{84} solids with La@C_{82} were indexed to face centre cubic (fcc) with a rhombohedral distortion. This distortion is similar to previous

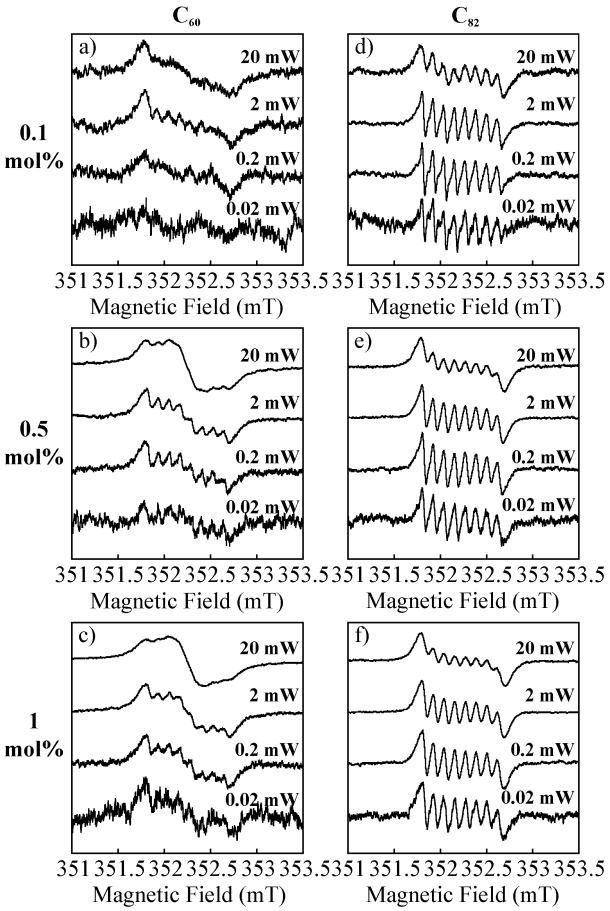

Fig. 4 Microwave power dependence of the ESR spectra of La@C_{82} in (a) 0.1; (b) 0.5; (c) 1 mol% in C_{60} matrix; (d) 0.1; (e) 0.5; (f) 1 mol% in C_{82} matrix at room temperature. Microwave frequency and modulation amplitude are 9.867 GHz and 0.025 mT, respectively.

observations in Fe-doped C_{70} crystals.[32] No influence of the amount of La@C_{82} on the crystal structure of C_{78} and C_{84} was observed. This suggests that La@C_{82} molecules are well dispersed in C_{78} and C_{84} matrices. However, the crystal structures of C_{60} and C_{82} with La@C_{82} were different between 0.1 and 1 mol% concentrations, indicating that the presence of La@C_{82} modifies the inherent crystal structure being formed. The diffraction pattern of C_{60} solid with 0.1 mol% La@C_{82} was indexed to fcc. On the other hand, C_{60} solid with 1 mol% La@C_{82} formed hexagonal closed packing (hcp). Our ESR measurements showed that La@C_{82} molecules form clusters in the C_{60} matrix. According to previous studies, M@C_{82} MFs can form not only fcc but also hcp structures. The solubilities of C_{60} and La@C_{82} in CS_2 are $\sim$7 mg ml^{-1} and less than 1 mg ml^{-1}, respectively. In highly concentrated C_{60}/1mol% La@C_{82} CS_2 solution, if a La@C_{82} molecule is close to another La@C_{82} molecule, the La@C_{82} molecules form a cluster because the amount of CS_2 molecule is not enough for La@C_{82} to be isolated. However C_{60} molecules do not crystallize because of the high solubility to CS_2 and the weak interaction between C_{60} molecules (only van der Waals interaction). Therefore La@C_{82} molecules crystallize faster than C_{60}. The hcp-La@C_{82} clusters may affect the crystal growth of C_{60} molecules by acting as crystal seeds. In the case

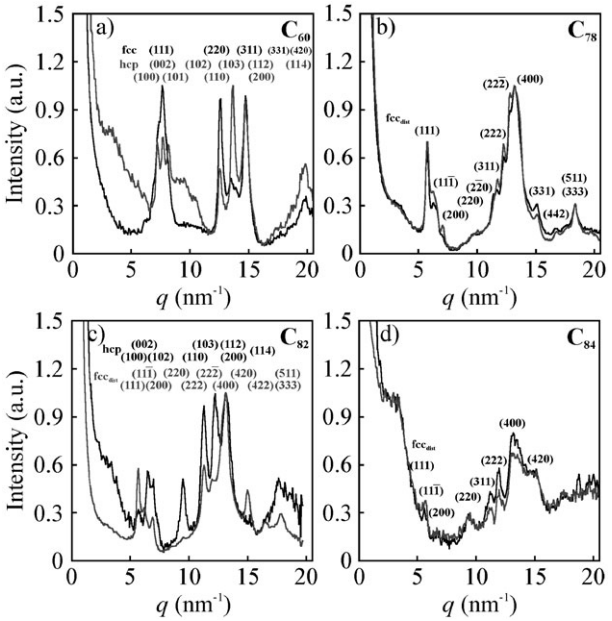

Fig. 5 X-Ray diffraction patterns of La@C_{82} in (a) C_{60}; (b) C_{78}; (c) C_{82}; and (d) C_{84} matrices at room temperature. Black and gray spectra show the diffraction pattern at 0.1 and 1 mol% concentrations of La@C_{82}, respectively.

of C_{82}, the diffraction patterns of C_{82} solid with 0.1 and 1 mol% La@C_{82} were indexed to hcp and rhombohedral-fcc, respectively.

Crystal structural analysis shows that La@C_{82} can be orientated in any direction within a rhombohedral-fcc-C_{82} solid. La@C_{82} in an hcp-C_{82} solid has restricted uniaxial rotation in the crystal. La@C_{82} molecules in the hcp-C_{82} can be ordered better than in the rhombohedral-fcc-C_{82}. The larger degrees of disorder in the rhombohedral-fcc (1 mol%) structure lead to increased inhomogeneous broadening in the ESR spectrum as compared to the hcp crystal structure. It is most likely that the change in the crystal structure of C_{82} arises from slight variations that may occur during the crystal formation process, such as rate of solvent evaporation. However, the conclusions drawn by correlating the XRD and ESR remain valid and show that variation in the crystal structure of the host matrix affects the spin properties of La@C_{82}.

4. Conclusions

We have investigated the ESR properties and crystal structures of solid-state La@C_{82} in various types of empty fullerene matrices. The dipole–dipole and exchange interactions between La@C_{82} molecules can be controlled by changing the concentration of La@C_{82} and the species of the empty fullerene matrix. The crystal structures of empty fullerenes containing trace quantities of La@C_{82} were measured using XRD and correlated with the ESR studies. The ordered nature of the hcp crystal structure of La@C_{82} in a C_{82} matrix leads to the narrowest linewidth of La@C_{82} in the solid state. The C_{60} matrix, used in earlier studies, has a low dispersion ability because of the large different solubility, resulting in clustering of La@C_{82} within the C_{60} matrix. We conclude that C_{82} is the best observed matrix for M@C_{82} type MFs in 3D arrays and propose that the diamagnetic (M_2C_2)@C_{82} type MFs[33,34] with the same cage structure as La@C_{82} may also be excellent matrices for dispersion.

Acknowledgements

This work has been supported by the Quantum Information Processing Interdisciplinary Research Collaboration (QIP IRC, EPSRC GR/S82176/01 and GR/S15808/01), and the Intra-Molecular Propagation of Electron Spin States (IMPRESS) project (EP/D074398/1, 05-FONE-FP002 and FWF I83-N20). JJLM and AA are supported by the Royal Society.

References

1 H. Shinohara, *Rep. Prog. Phys.*, 2000, **63**, 843.
2 T. A. Murphy, T. Pawlik, A. Weidinger, M. Hohne, R. Alcala and J. M. Spaeth, *Phys. Rev. Lett.*, 1996, **77**, 1075.
3 J. J. L. Morton, A. M. Tyryshkin, A. Ardavan, S. C. Benjamin, K. Porfyrakis, S. A. Lyon and G. A. D. Briggs, *Nat. Phys.*, 2006, **2**, 40.
4 T. Kato, S. Suzuki, K. Kikuchi and Y. Achiba, *J. Phys. Chem.*, 1993, **97**, 13425.
5 N. Okabe, Y. Ohba, S. Suzuki, S. Kawata, K. Kikuchi, Y. Achiba and M. Iwaizumi, *Chem. Phys. Lett.*, 1995, **235**, 564.
6 S. Knorr, A. Grupp, M. Mehring, U. Kirbach, A. Bartl and L. Dunsch, *Appl. Phys. A: Mater. Sci. Process.*, 1998, **66**, 257.
7 C. Knapp, K. P. Dinse, B. Pietzak, M. Waiblinger and A. Weidinger, *Chem. Phys. Lett.*, 1997, **272**, 433.
8 E. Dietel, A. Hirsch, B. Pietzak, M. Waiblinger, K. Lips, A. Weidinger, A. Gruss and K. P. Dinse, *J. Am. Chem. Soc.*, 1999, **121**, 2432.
9 J. J. L. Morton, A. M. Tyryshkin, A. Ardavan, K. Porfyrakis, S. A. Lyon and G. A. D. Briggs, *J. Chem. Phys.*, 2005, **122**, 174504.
10 R. Kitaura and H. Shinohara, *Chem.–Asian J.*, 2006, **1**, 646.
11 J. H. Warner, Y. Ito, M. Zaka, L. Ge, T. Akachi, H. Okimoto, K. Porfyrakis, A. A. R. Watt, H. Shinohara and G. A. D. Briggs, *Nano Lett.*, 2008, **8**, 2328.
12 T. Nagano, E. Kuwahara, T. Takayanagi, Y. Kubozono and A. Fujiwara, *Chem. Phys. Lett.*, 2005, **409**, 187.
13 H. Shinohara, H. Sato, M. Ohkohchi, Y. Ando, T. Kodama, T. Shida, T. Kato and Y. Saito, *Nature*, 1992, **357**, 52.
14 C. S. Yannoni, M. Hoinkis, M. S. Devries, D. S. Bethune, J. R. Salem, M. S. Crowder and R. D. Johnson, *Science*, 1992, **256**, 1191.
15 M. Rubsam, P. Schweitzer and K. P. Dinse, *J. Phys. Chem.*, 1996, **100**, 19310.
16 M. Inakuma and H. Shinohara, *J. Phys. Chem. B*, 2000, **104**, 7595.
17 J. H. Weaver, Y. Chai, G. H. Kroll, C. Jin, T. R. Ohno, R. E. Haufler, T. Guo, J. M. Alford, J. Conceicao, L. P. F. Chibante, A. Jain, G. Palmer and R. E. Smalley, *Chem. Phys. Lett.*, 1992, **190**, 460.
18 H. Shinohara, H. Sato, Y. Saito, M. Ohkohchi and Y. Ando, *J. Phys. Chem.*, 1992, **96**, 3571.
19 Y. Chai, T. Guo, C. M. Jin, R. E. Haufler, L. P. F. Chibante, J. Fure, L. H. Wang, J. M. Alford and R. E. Smalley, *J. Phys. Chem.*, 1991, **95**, 7564.
20 R. D. Johnson, M. S. Devries, J. Salem, D. S. Bethune and C. S. Yannoni, *Nature*, 1992, **355**, 239.
21 D. S. Bethune, R. D. Johnson, J. R. Salem, M. S. Devries and C. S. Yannoni, *Nature*, 1993, **366**, 123.
22 N. Weiden, T. Kato and K. P. Dinse, *J. Phys. Chem. B*, 2004, **108**, 9469.
23 C. J. Nuttall, Y. Inada, K. Nagai and Y. Iwasa, *Phys. Rev. B: Condens. Matter Mater. Phys.*, 2000, **62**, 8592.
24 Y. Ito, W. Fujita, T. Okazaki, T. Sugai, K. Awaga, E. Nishibori, M. Takata, M. Sakata and H. Shinohara, *ChemPhysChem*, 2007, **8**, 1019.

25 C. J. Nuttall, Y. Hayashi, K. Yamazaki, T. Mitani and Y. Iwasa, *Adv. Mater.*, 2002, **14**, 293.
26 P. Jakes, A. Gembus, K. P. Dinse and K. Hata, *J. Chem. Phys.*, 2008, **128**, 052306.
27 K. Kikuchi, N. Nakahara, T. Wakabayashi, S. Suzuki, H. Shiromaru, Y. Miyake, K. Saito, I. Ikemoto, M. Kainosho and Y. Achiba, *Nature*, 1992, **357**, 142.
28 T. J. S. Dennis, T. Kai, K. Asato, T. Tomiyama, H. Shinohara, T. Yoshida, Y. Kobayashi, H. Ishiwatari, Y. Miyake, K. Kikuchi and Y. Achiba, *J. Phys. Chem. A*, 1999, **103**, 8747.
29 Y. Saito, N. Fujimoto, K. Kikuchi and Y. Achiba, *Phys. Rev. B: Condens. Matter*, 1994, **49**, 14794.
30 S. Stoll and A. Schweiger, *J. Mag. Res.*, 2006, **178**, 42.
31 R. Wilson and D. Kivelson, *J. Chem. Phys.*, 1966, **44**, 154.
32 K. Misof, P. Fratzl and G. Vogl, *Europhys. Lett.*, 1993, **22**, 585.
33 T. Inoue, T. Tomiyama, T. Sugai, T. Okazaki, T. Suematsu, N. Fujii, H. Utsumi, K. Nojima and H. Shinohara, *J. Phys. Chem. B*, 2004, **108**, 7573.
34 H. Okimoto, W. Hemme, Y. Ito, T. Sugai, R. Kitaura, H. Eckert and H. Shinohara, *Nano*, 2008, **3**, 21.